Characterization of Ordered Mesoporous Gallium MCM-41 Synthesized at Room Temperature

M. Chatterjee,* T. Iwasaki, Y. Onodera, T. Nagase, H. Hayashi, and T. Ebina

Inorganic Materials Section, Tohoku National Industrial Research Institute, 4-2-1 Nigatake, Miyagino-ku, Sendai 983-8551, Japan

Received November 23, 1999. Revised Manuscript Received February 17, 2000

A series of highly ordered mesoporous gallium-containing MCM-41 molecular sieves with variable Si/Ga (100−10) ratios have been synthesized at room temperature. The synthesized Ga−MCM-41 was investigated by powder X-ray diffraction, transmission electron microscopy, thermal analysis, N_2 adsorption measurement, and ^{29}Si and ^{71}Ga nuclear magnetic resonance (NMR); optimal synthesis conditions have thus been established. We were successful in synthesizing highly ordered material at room temperature using gallium nitrate as the source of gallium, and the surfactant was the cetyltrimethylammonium cation $[(C_{16}H_{33}N(CH_3)_3]^+$. ^{71}Ga NMR of calcined and uncalcined Ga−MCM-41 demonstrated that gallium was substituted for Si with tetrahedral coordination in the Ga−MCM-41 structure. N_2 adsorption measurements indicate that high mesoporosity exists over the entire range of Ga−MCM-41 with an average pore diameter of 38.3 Å.

Introduction

The mesoporous molecular sieve MCM-41 (a member of the M41S family), which possesses a hexagonally arranged uniform pore structure, was discovered by Beck et al. in 1992.[1] The important characteristics of this novel material are its large BET surface area, high porosity, and controllable and narrowly distributed pore sizes. Those characteristics manifest themselves as a very promising candidate as catalyst, catalyst support,[2−4] and adsorbent.[5−7] It may act as host (for host−guest encapsulation) to develop advanced composite materials.[8,9] Among the different members of the M41S family, MCM-41 exhibits a hexagonal array of uniform mesopores that has been the focus of most studies. Beginning with a relatively inert all-silica MCM-41, great chemical and catalytic diversity may be generated by isomorphous substitution. For example, isomorphous substitution with trivalent cations such as Al^{3+}, B^{3+}, Ga^{3+}, and Fe^{3+} is accompanied by the formation of Brønsted acid sites. There is no doubt that the presence of these very large pores combined with acidic properties opens up new possibilities for processing and/or producing large molecules. The isomorphous substitution of gallium in various zeolites is well established.[10−12] The synthesis and characterization of gallosilicate analogues of faujasite[13] and analcite[14] were well documented. MFI-type gallosilicates have been proved to have excellent activity for the aromatization of hydrocarbons.[15] The introduction of gallium into silicates or aluminosilicates resulted in high selectivity to aromatics in the catalytic conversion of olefins and paraffins.[16−19]

The substitution of silicon by gallium during the synthesis of MCM-41 was expected to modify the acidic properties as well as catalytic properties of these materials. Cheng et al.[20,21] have reported the hydrothermal synthesis and characterization of the gallium-containing mesoporous molecular sieve MCM-41. They have carried out the synthesis at 150 °C for 3 days. In as-synthesized and noncalcined samples, gallium is 4-coordinated and forms a part of the MCM-41 structure. Takeguchi et al.[22] described the hydrothermal

---

* Corresponding author. E-mail maya@tniri.go.jp; telephone 81-22-237-5211; FAX 81-22-236-6839.

(1) Beck, J. S.; Vartuli, J. C.; Roth, W. J.; Leonowicz, M. E.; Kresege, C. T.; Schmitt, K. D.; Chu, C. T.-W.; Olsen, D. H.; Sheppard, E. W.; McCullen, S. C.; Higgins, J. B.; Schlenker, J. L. *J. Am. Chem. Soc.* **1992**, *114*, 10834.

(2) Kloetstra, R. K.; van Bekkum, H. *J. Chem. Res.* **1995**, 26.

(3) (a) Corma, A.; Martínez, A.; Martínez-Soria, V.; Montón, J. B. *J. Catal* **1995**, *153*, 25. (b) Corma, A.; Navarro, M. T.; Pariente, J. P. *J. Chem. Soc., Chem. Commun.* **1994**, 147.

(4) Sayari, A. *Chem. Mater.* **1996**, *8*, 1840.

(5) Branton, P. J.; Hall, P. G.; Sing, K. S. W. *J. Chem. Soc., Chem. Commun.* **1993**, 1257.

(6) Rathousky, J.; Zukai, A.; Franke, O.; Schulz-Ekloff, G. *J. Chem. Soc., Faraday Trans.* **1994**, *90*, 2821.

(7) Ioneva, M. A.; Newman, G.K.; Harwell, J. H. In *Novel Adsorbents and their Environmental Applications*; *AIChE Symp. Ser.* **1995**, *91*, 40.

(8) (a) Wu, C. G.; Bein, T. *Science* **1994**, *266*, 1013. (b) Wu, C. G.; Bein, T. *Science* **1994**, *264*, 1757. (c) Wu, C. G.; Bein, T. *Chem. Mater.* **1994**, *6*, 1109.

(9) Huber, C.; Moller, K.; Bein, T. *J. Chem. Soc., Chem. Commun.* **1994**, 2619.

(10) Barrer, R. M.; Brynman, J. M.; Bultitude, F. W.; Meier, W. M. *J. Chem. Soc.* **1959**, 195.

(11) Barrer, R. M.; Dicks, L. W. R. *J. Chem. Soc. A* **1966**, 1379.

(12) Suzuki, K.; Kiyozumi, Y.; Shin, S. S.; Ueda, S. *Zeolites* **1985**, *5*, 11.

(13) Selbin, J.; Mason, R.B. *J. Inorg. Nucl. Chem.* **1961**, *20*, 222.

(14) Aust. Pat. 18634.

(15) Lalik, E.; Liu, X.; Klinowski, J. *J. Phys. Chem.* **1992**, *96*, 805.

(16) Singh, A. P.; Reddy, K. R. *Zeolites* **1994**, *14*, 291.

(17) Giannetto, G.; Monque, R.; Galiasso, R. *Catal. Rev.*−*Sci. Eng.* **1994**, *36*, 271.

(18) Ono, Y. *Catal. Rev.*−*Sci. Eng.* **1992**, *34*, 179.

(19) Inui, T.; Makino, Y.; Okazumi, F.; Nagase, S.; Miyamoto, A. *Ind. Eng. Chem. Res.* **1987**, *26*, 647.

(20) Cheng, C.; He, H.; Zhou, W.; Klinowski, J.; Goncalves, J. A. S.; Gladden, L. F. *J. Phys. Chem.* **1996**, *100*, 390.

(21) Cheng, C.; Klinowski, J. *J. Chem. Soc., Faraday Trans.* **1996**, *92*, 289.

(22) Takeguchi, T.; Kim, J.; Kang, M.; Inui, T.; Cheuh, W.; Haller, L. G. *J. Catal.* **1998**, *175*, 1.

10.1021/cm990739b CCC: $19.00

Table 1. Analytical Data

sample	Si/Ga gel	Si/Ga products	d_{100} (calcined Ga−MCM-41) (Å)	surf. area ($m^2\ g^{-1}$)	APD[a] (Å)	a_0[b] (Å)	av pore wall thickness (Å)
1	100	95.3	36.8	975	35.2	42.4	7.2
2	50	52.6	39.8	861	37.6	46.0	8.4
3	20	22.8	40.7	815	38.3	47.0	8.7
4	10	13.5	39.4	703	36.6	48.5	11.9
5	∞		33.5			38.6	

[a] APD = average pore diameter. [b] a_0 = the lattice parameter calculated from XRD data using the formula $a_0 = 2d_{100}/\sqrt{3}$. Pore wall thickness (Å) = a_0 − APD.

synthesis of alkali-free gallium-substituted MCM-41, but the XRD pattern of most of their samples showed lower ordering.

We report on a series of gallium-substituted MCM-41 mesoporous materials synthesized at room temperature using gallium nitrate as the source of gallium and tetraethyl orthosilicate as the silica source. XRD, N_2 adsorption, transmission electron microscopy (TEM), thermal analysis, ^{71}Ga magic angle spinning (MAS) NMR, and ^{29}Si magic angle spinning (MAS) NMR characterized the products. The material can act as a potential catalyst in the aromatization reaction. Its higher surface area and larger channels make the diffusion of larger organic molecule faster. It is the purpose of the article to report an easy method for the synthesis of highly ordered Ga−MCM-41 at room temperature. The effect of the gallium content on the acidity was examined by characterization of Ga−MCM-41.

Experimental Section

Synthesis. The synthesis of Ga−MCM-41 was carried out using gels with the following molar composition: SiO_2:$x$$Ga_2O_3$:0.1($C_{16}H_{33}N\ (CH_3)_3Br$:0.23$Na_2O$:107$H_2O$. The gel mixture was prepared using tetraethyl orthosilicate (TEOS) (Nacalai Tesque Inc. Japan), gallium(III) nitrate hydrate (99%, Aldrich), cetyltrimethylammonium bromide (Merck), sodium hydroxide, and deionized water.

The synthesis procedure was as follows. A 0.874 g sample of cetyltrimethylammonium bromide was added to the deionized water and stirred until a clear solution was obtained. The required amount of gallium nitrate was dissolved in water and then slowly added to the solution of surfactant; stirring was continued until homogeneity was achieved. Then a solution of sodium hydroxide was added to the mixture, and the mixture was stirred for an hour. To this clear solution was added 5 g of TEOS under stirring conditions, and the pH was maintained at 11.3. After stirring for about 24 h, a white solid was formed. The resultant product was washed thoroughly with deionized water. The sample was dried exclusively at room temperature before characterization. The organic matter was removed by calcining the sample at 600 °C for 8 h.

Sample Characterization Techniques. *Chemical Analyses*. Chemical analysis was performed by a SPS 1500R plasma spectrometer.

X-ray Diffraction. X-ray diffraction patterns were recorded using a Rigaku-RAD-X system using monochromatized Cu Kα radiation (40 kV, 20 mA), 0.020° step size.

N_2 Adsorption Measurement. N_2 adsorption measurements were carried out using a Micromeritics ASAP 2400 analyzer. The volume of adsorbed N_2 was normalized to standard temperature and pressure. Before the experiments, samples were degassed at 300 °C for one night. The specific surface area, A_{BET}, was determined from the linear part of the BET plot (p/p_0 = 0.05−0.30). The mesopore size distribution (PSD) was calculated using desorption branches of the N_2 adsorption isotherm and the Barrett−Joyner−Halenda (BJH) formula as suggested by Tanev et al.[23]

Transmission Electron Microscopy (*TEM*). Calcined samples were deposited on a grid with a holey carbon copper film and rapidly transferred to a JEOL JEM-2000EX (II) operating at 200 kV. The sample was then kept in the microscope vacuum (5×10^{-7} T). TEM images were recorded at magnifications of ×100 000.

Thermogravimetric Analysis. TG analysis was carried out by using a Rigaku Thermoflex TAS200 unit. About 10 mg of the sample was placed in a platinum pan and was heated at a heating rate of 10 °C/min.

Solid-State NMR. ^{71}Ga and ^{29}Si NMR spectra were recorded at 11.75 T on a Varian INOVA 500 NMR spectrometer with CPIMS probes. The ^{29}Si MAS spectrum was measured at 99.3 MHz using a SiN rotor at 3 kHz. ^{71}Ga spectra were acquired at 152.5 MHz with 8.0 μs pulse length, recycling time 1.000 s, and a SiN rotors 5 mm in diameter without spinning and with spinning at 10 kHz. The chemical shifts were given in ppm using tetramethylsilane (TMS) as external reference for ^{29}Si NMR, and for ^{71}Ga NMR usually 1 M aqueous $Ga(NO_3)_3$ solutions were chosen as external reference sample to determine the signal position $\delta([M(H_2O)_6]^{3+}) = 0$ ppm. All spectra were recorded at room temperature.

Results and Discussion

Elemental Analysis. The elemental analyses of the solid products as determined by ICAES are summarized in Table 1. The ratio of Si/Ga in the product was very close to that in the gel, indicating an incorporation of gallium in the resultant solid.

Powder X-ray Diffraction. The XRD patterns of Ga−MCM-41 samples are shown in Figure 1. Most of the Ga−MCM-41 samples have four peaks. The better resolution of (100), (110), (200), and (210) peaks corresponds to the high crystallinity of Ga−MCM-41. All four XRD reflections can be indexed on a hexagonal lattice. According to the subsequent literature,[24] the XRD pattern of room-temperature-synthesized Si−MCM-41 was short- to medium-range hexagonal ordering with relatively low intensity of the (100) diffraction peak and very poor resolution of higher order peaks. The material prepared by our method showed a highly resolved XRD peak. Hence, ordered mesoporous material can be obtained at room temperature also. After calcination of the as-made product the intensity of the XRD peak increases which is due to the removal of the intercalated organic compounds. The shifting of the peak position was also observed in the calcined samples. This shifting of the peak position corresponds to a lattice contraction of ∼10.5%. According to Chen et al.,[25] after calcination lattice contraction could be of 25% (depending on the method of synthesis) in the case of Si−MCM-41. Table 1 lists the d_{100} spacing and hexagonal unit cell parameters (a_0). From Table 1 it has been found that the unit cell parameters a_0 [calculated from (100) peak] of Ga−

---

(23) Tanev, P. T.; Vlaev, L. T. *J. Colloid Interface Sci.* **1993**, *160*, 110.

(24) Tanev, P. T.; Pinnavia, T. J. *Chem. Mater.* **1996**, *8*, 2068.

(25) Chen, C. Y.; Li, H. X.; Davis, M. E. *Microporous Mater.* **1993**, *2*, 17.

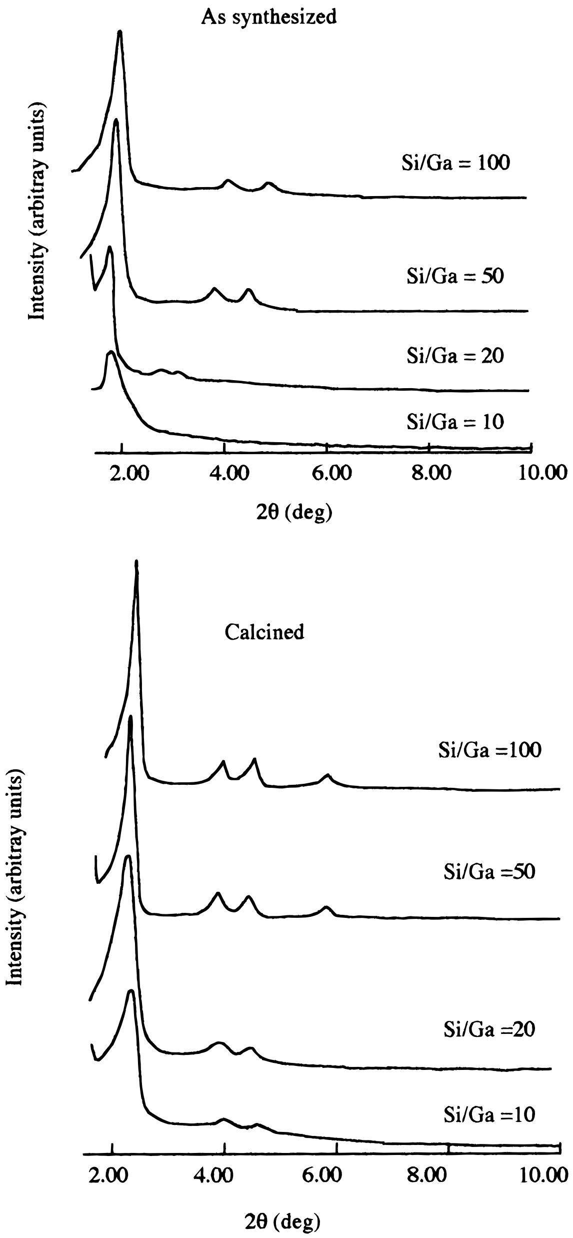

Figure 1. X-ray diffraction patterns of (a) as-synthesized and (b) calcined Ga−MCM-41 (Si/Ga = 100−10) samples.

MCM-41 increased in comparison to that of their pure silica analogue. This observation confirms the presence of gallium in the framework. With increasing gallium content, the unit cell parameter (a_0) of Ga−MCM-41 (Si/Ga = 100−10) does not increase as much as we expected from Al−MCM-41. The bond length of Ga−O is longer than Si−O which should increase the repeat distance in Ga−MCM-41, but the Ga−O−Si bond angle decreased with increasing gallium content. The effect of increase in bond length and decrease in bond angle played a dominating role in the variations of the repeat distances.

The XRD patterns of the calcined and uncalcined material show hexagonal lattice structure, which confirms the structural stability of the Ga−MCM-41, following removal of the structure-directing surfactant molecules. X-ray diffraction, however, does not provide any direct evidence regarding the extent to which gallium has been incorporated into the framework. So, other techniques should be used to characterize the solid material.

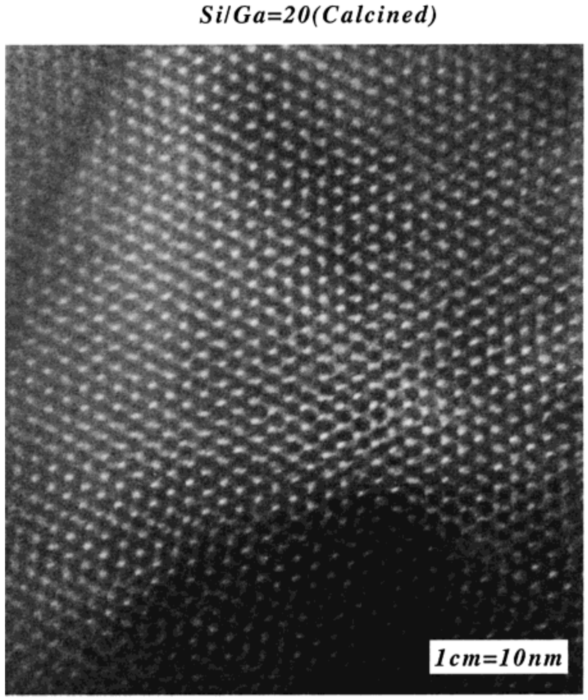

Figure 2. TEM photograph of calcined Ga−MCM-41 (Si/Ga = 20) sample.

Transmission Electron Microscopy. The uniform mesopore structure of Ga−MCM-41 is evident in the transmission electron microscope lattice image (Si/Ga = 20) shown in Figure 2. TEM of the calcined sample shows a regular hexagonal array of uniform channels which is characteristic of MCM-41. The hexagonal structure with each pore surrounded by six neighbors was present in all samples. It confirms the occurrence of well-ordered hexagonal structure. This is entirely consistent with the XRD results.

Thermal Analysis. The thermal analysis pattern of Ga−MCM-41 (shown in Figure 3) was very similar to that of Si−MCM-41. Total weight loss occurs at three distinctive steps (TG curves). Step 1 was associated with physically adsorbed water constituting about 6% weight loss. Step 2 was related to the decomposition of the template (Hoffmann elimination reaction $C_{16}H_{33}(CH_3)_{3N}^{+} \rightarrow C_{16}H_{32} + N(CH_3)_3 + H^+$) with 28% of the weight loss. Step 3 directed the combustion of the remaining organic ions. A sharp DTA peak is observed both for Si−MCM-41 and Ga−MCM-41 around 300 °C. This sharp peak is attributed to the strong exothermic process due to the combustion and removal of the surfactant from the mesopores of the MCM-41. A small shoulder around 340 °C is also observed in the DTA curve of Ga−MCM-41. As this shoulder does not appear in the Si−MCM-41, the results show some higher temperature is required to remove some of the surfactant. This result indicates some interaction between occluded surfactant and framework gallium.[26] On summarizing, the thermoanalytical data confirm that Ga−MCM-41 is a highly porous material, and their rapid weight loss confirms the openness of the pore system.

---

[26] Busio, M.; Janchan, J.; van Hoff, J. H. C. *Microporous Mater.* **1995**, *5*, 211.

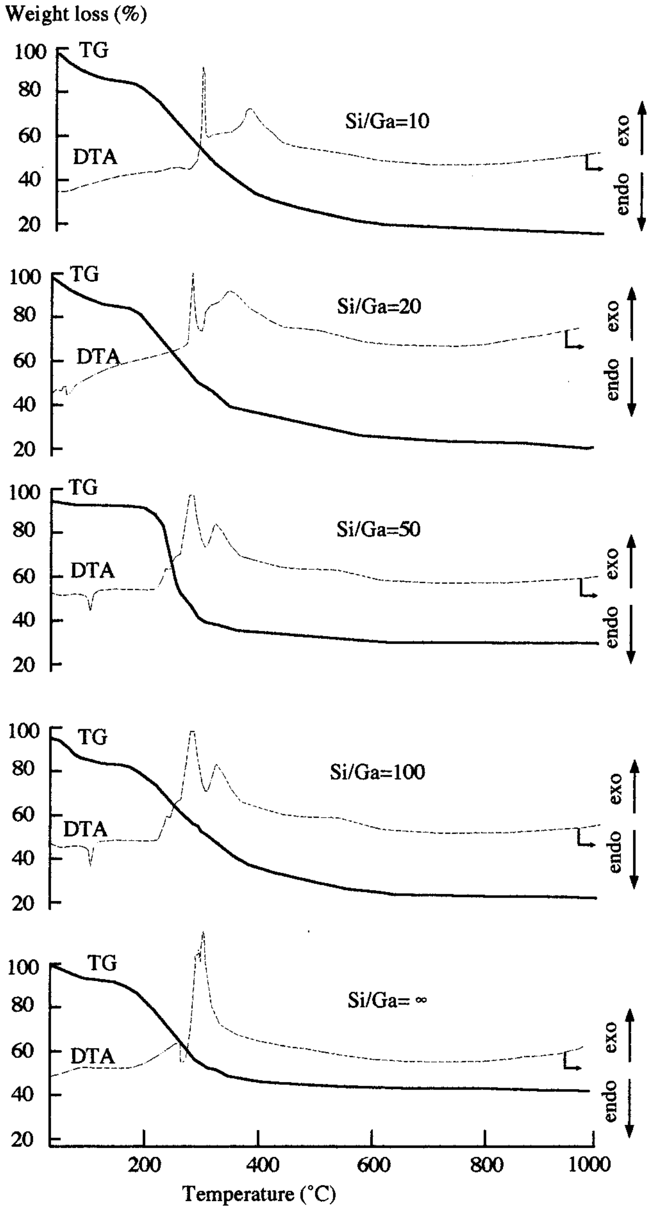

Figure 3. Thermal analysis pattern of as-synthesized Ga−MCM-41 (Si/Ga = 100−∞).

N_2 Adsorption Isotherm. The N_2 adsorption−desorption isotherm is presented in Figure 4a. These type IV isotherms are typical of MCM-41 mesoporous solids. The inflection in the adsorption isotherm at $p/p_0 < 0.3$ indicates the mesopore filling and does not imply the micropores. The N_2 sorption isotherm of the Ga−MCM-41 meso structure was characterized by an adsorption step at a relative pressure $p/p_0 = 0.35$ due to capillary condensation. At $p/p_0 > 0.3$ the isotherms exhibit a sharp inflection point which is related to the diameter of the mesopore. The sharpness in this step suggests uniformity in the pore size of Ga−MCM-41[27] synthesized at room temperature. Furthermore, that the initial region can be extrapolated back to the origin confirms the absence of any detectable micropore filling at low p/p_0.

A plot of the derivative of the pore volume per unit weight concerning the pore diameter (d*V*/d*D*) is shown in Figure 4b. The pore size distribution curve of higher gallium content material [Ga−MCM-41 (10)] shows that it has a narrow pore size distribution, and no macropores are formed with a broad range of pore diameters. The BET surface area of Ga−MCM-41 (20) was close to 815 $m^2\ g^{-1}$, and the average pore diameter is 38.3 Å.

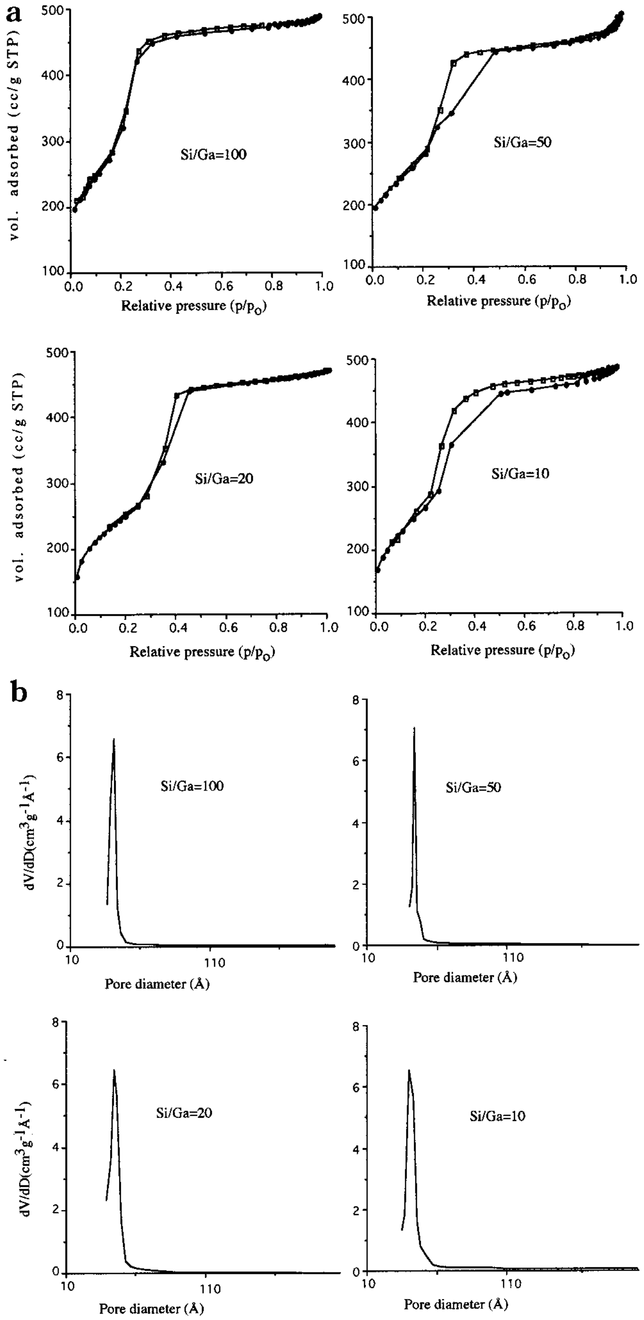

Figure 4. N_2 adsorption−desorption (a) isotherm and (b) pore size distribution of calcined sample (Si/Ga = 100−10).

^{71}Ga MAS NMR. ^{71}Ga MAS NMR spectra of as-made and calcined Ga−MCM-41 samples are shown in Figure 5, a and b, respectively. Each as-synthesized Ga−MCM-41 has a peak around +147 ppm. A peak in this region had earlier been observed in other gallosilicate structure and was identified as originating from 4-coordinated tetrahedral gallium present in the framework.[28] Gallium with octahedral coordination was not observed in any

---

(27) Branton, P. J.; Hall, P. G.; Sing, K. S. W.; Reichert, H.; Schöth, F.; Unger, K. K. *J. Chem. Soc., Faraday Trans.* **1994**, *90*, 2965.

(28) Timken, H. K. C.; Oldfield, E. *J. Am. Chem. Soc.* **1987**, *109*, 7669.

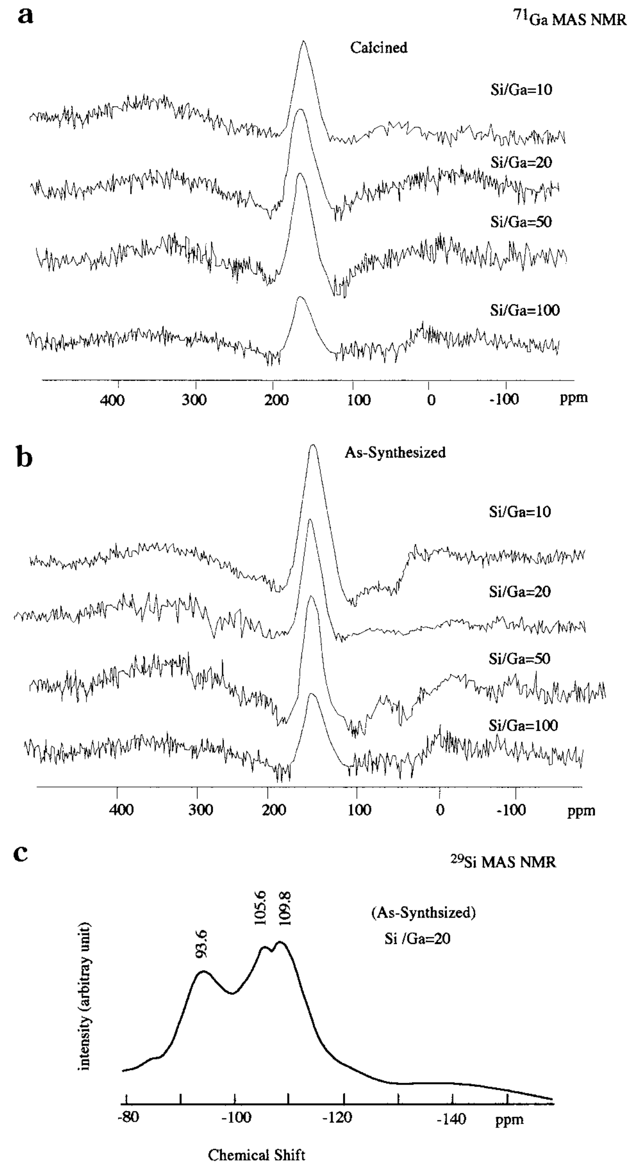

Figure 5. ^{71}Ga MAS NMR spectra of (a) as-synthesized and (b) calcined Ga−MCM-41(Si/Ga = 100−10) and (c) ^{29}Si MAS NMR spectra of Ga−MCM-41 (as-synthesized).

of the as-synthesized samples. The intensity of the +147 ppm peak increases with increase of gallium content. After calcination the resonance shifted to +153 ppm. None of the calcined Ga−MCM-41 shows any resonance near ~0 ppm where hexahydrated octahedral gallium $Ga(H_2O)_{63}^{+}$ was expected. After calcination the tetrahedral resonance peak of Ga−MCM-41 of higher gallium content (Si/Ga = 10) suffered a little decrease in intensity. According to Bayense et al.,[29,30] concentration of framework gallium can be measured by NMR reliably from the quantitative determination of the resonance peak area, but the 6-coordinated gallium cannot be detected. Cheng et al.[19] described that the concentration of 6-coordinated gallium can be estimated by ^{71}Ga NMR from the decrease in peak intensity of the 4-coordinated gallium line. Therefore, little decrease in intensity of the tetrahedral resonance line of higher gallium-containing sample indicates the possibility of finding tetrahedral and octahedral gallium. Hence, it can be concluded that the incorporation of gallium in the tetrahedral position of the MCM-41 structure can be achieved.

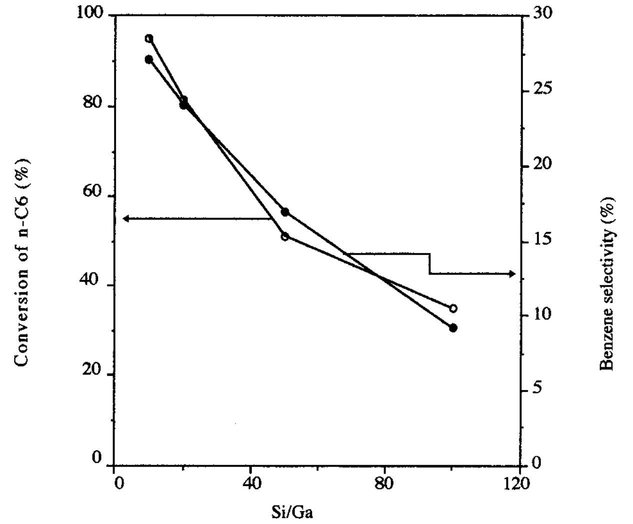

Figure 6. Effect of gallium content upon aromatization of *n*-hexane (Si/Ga = 100−10).

^{29}Si MAS NMR. The framework of mesoporous M41S differs from that of microporous zeolites of three-dimensional tetrahedral network. It closely resembles amorphous silica, suggesting a broad range of Si−O−Si bond angles. ^{29}Si MAS NMR spectra (Figure 5c) of as-synthesized Ga−MCM-41 sample consist of some broad peaks at −110, −105.6, and −93.6 ppm with respect to TMS. Indeed, the ^{29}Si MAS NMR spectrum of siliceous MCM-41 exhibits three peaks at −92.4, −101.7, and −110.5 ppm.[31] The peak at −105.6 ppm may be assigned to the Si (1Ga) species by analogy to chemical shift observed on Ga−ZSM-5.[32] The results from ^{71}Ga and ^{29}Si NMR confirmed the presence of gallium in the framework structure of mesoporous material.

Catalytic Activity. That the gallium was incorporated into the framework positions has been evidenced from lattice expansion (Table 1). The other physicochemical techniques adopted validate the incorporation. Now, to justify the incorporation, here we have carried out the aromatization of *n*-hexane (Figure 6). It has been found that with increase in gallium content the total conversion increases. ^{71}Ga NMR demonstrated that a part of gallium has been expelled from the structure of higher gallium content materials. Hence, Ga−MCM-41 (Si/Ga < 20) contains both framework and extrframework gallium. So, framework or extraframework gallium should be the active site for *n*-hexane aromatization. As with increasing gallium content the rate of formation of benzene does not increase considerably, we can conclude that the significant catalytic activity of Ga−MCM-41 is due to the framework gallium, which can act as an active site in the aromatization reaction.

---

(29) Bayense, C. R.; van Hooff, J. H. C.; Kentgens, A. P. M.; de Hann, J. W.; van de Van, L. J. M. *J. Chem. Soc., Chem. Commun.* **1989**, 1292.

(30) Bayense, C. R.; Kentgens, A. P. M.; de Hann, J. W.; van de Van, L. J. M.; van Hooff, J. H. C. *J. Phys. Chem.* **1992**, *96*, 775.

(31) Sindorf, D. W.; Maciel, G. E. *J. Am. Chem. Soc.* **1981**, *103*, 4263.

(32) Khodakov, A. Y.; Kustov, L. P.; Bendarenko, T. N.; Dargachev, A. A.; Kazansky, V. B.; Minachev, Kh. M.; Borbély, G.; Beyer, H. K. *Zeolites* **1990**, *10*, 603.

Conclusion

The gallium analogue of mesoporous MCM-41 with hexagonal structure can be synthesized with relatively high gallium contents at room temperature (by the easiest method). Chemical analysis confirms the presence of gallium in the product. The resultant material is thermally stable. Characterization of the material by XRD indicates the higher crystallinity of the material. N_2 adsorption reveals a uniformity in the mesopore structure and high surface area. TEM of different samples indicates a regular hexagonal ordering. ^{71}Ga NMR confirms the incorporation of gallium in the tetrahedral position. This class of Ga−MCM-41 materials shows high selectivity to aromatics in the catalytic conversion of hexane.

Acknowledgment. M.C. gratefully acknowledges the financial support from the AIST of Japan.

CM990739B